RSC Advances

PAPER

View Article Online
View Journal | View Issue

Cite this: *RSC Adv.*, 2024, **14**, 1527

Enhancing osteogenic differentiation of MC3T3-E1 cells during inflammation using UPPE/β-TCP/TTC composites *via* the Wnt/β-catenin pathway†

Qi-lin Li,[abc] Ya-xin Wu,[abc] Yu-xiao Zhang,[abc] Jing Mao *[abc] and Zhi-xing Zhang *[abc]

Periodontitis can lead to defects in the alveolar bone, thus increasing the demand for dependable biomaterials to repair these defects. This study aims to examine the pro-osteogenic and anti-bacterial properties of UPPE/β-TCP/TTC composites (composed of unsaturated polyphosphoester [UPPE], β-tricalcium phosphate [β-TCP], and tetracycline [TTC]) under an inflammatory condition. The morphology of MC3T3-E1 cells on the composite was examined using scanning electron microscopy. The toxicity of the composite to MC3T3-E1 cells was assessed using the Alamar-blue assay. The pro-osteogenic potential of the composite was assessed through ALP staining, ARS staining, RT-PCR, and WB. The antimicrobial properties of the composite were assessed using the zone inhibition assay. The results suggest that: (1) MC3T3-E1 cells exhibited stable adhesion to the surfaces of all four composite groups; (2) the UPPE/β-TCP/TTC composite demonstrated significantly lower toxicity to MC3T3-E1 cells; and (3) the UPPE/β-TCP/TTC composite had the most pronounced pro-osteogenic effect on MC3T3-E1 cells by activating the WNT/β-catenin pathway and displaying superior antibacterial properties. UPPE/β-TCP/TTC, as a biocomposite, has been shown to possess antibacterial properties and exhibit excellent potential in facilitating osteogenic differentiation of MC3T3-E1 cells.

Received 14th August 2023
Accepted 19th December 2023

DOI: 10.1039/d3ra05529a

rsc.li/rsc-advances

1. Introduction

Periodontitis is an inflammatory disease caused by interacting with specific bacterial pathogens, herpesviruses, and other oral pathogenic microorganisms.[1] Periodontitis gradually deteriorates the periodontal membranes, alveolar bone, and teeth, ultimately resulting in their destruction.[2,3] Reconstructing periodontal bone defects and achieving periodontal regeneration remains a major challenge in regenerative medicine.[4] Periodontal bone defects are traditionally treated by employing suitable bone substitutes to fill the defect and guide bone regeneration.[5] However, current biomaterials for bone regeneration have several disadvantages. Firstly, the bio-degradation of implanted materials is unsatisfactory.[6] Secondly, there is instability in drug release from these biomaterials.[7] Finally, placing biomaterials into the periodontal pocket is typically technically challenging and time-consuming.[8] Therefore, developing injectable and biodegradable biomaterials is crucial for effectively treating periodontal bone defects.

Periodontal bone defects, particularly load-bearing, have been repaired internally with biodegradable artificial bone substitutes.[9] Recent studies have demonstrated that the incorporation of biocompatible fillers, such as hydroxyapatite (HA) or calcium phosphate (CP), into macromolecular polymers can form an organic–inorganic composite material exhibiting enhanced mechanical properties and bioactivities.[10] Previous research has demonstrated the exceptional biocompatibility and bone conductivity of β-tricalcium phosphate (β-TCP), which allows for its absorption and replacement by new bone tissue. Unlike other glassy fillers, β-TCP powders function as fillers within the complex, facilitating the release of calcium and phosphate ions. This mechanism further promotes the mineralization of new bone and demineralized dentin.[11] Tetracycline (TTC) and its non-antibiotic chemo-isomeric derivatives have special pharmacological activities, mainly including inhibiting the expression of metalloproteinases, inhibiting bone resorption, restoring the structure and function of osteoblasts, and the above properties have essential application in regenerative medicine.[12–14] Studies have shown that low concentration of TTC hydrochloride can promote the activity and proliferation capacity of human embryonic osteoblasts cultured *in vitro* and increase the synthesis of preformed collagen, osteocalcin, and other bone substances, suggesting that tetracycline has a solid

[a]*Department of Stomatology, Tongji Hospital, Tongji Medical College, Huazhong University of Science and Technology, Wuhan 430030, China. E-mail: maojing@hust.edu.cn; zzx@tjh.tjmu.edu.cn*

[b]*School of Stomatology, Tongji Medical College, Huazhong University of Science and Technology, Wuhan 430030, China*

[c]*Hubei Province Key Laboratory of Oral and Maxillofacial Development and Regeneration, Wuhan 430022, China*

† Electronic supplementary information (ESI) available. See DOI: https://doi.org/10.1039/d3ra05529a

potential to promote bone defect repair.[15–17] The osteogenic differentiation of stem cells is frequently hindered by the persistent inflammatory and bacterial microenvironment characteristic of periodontitis, thereby exacerbating periodontal bone defects.[18,19] However, it remains uncertain whether the inclusion of TTC with UPPE/β-TCP materials improves the osteogenic differentiation potential of MC3T3-E1 cells within the periodontal inflammatory microenvironment, as well as the associated molecular mechanisms.

In this study, we introduced 1% TTC to the UPPE/β-TCP composite and assessed its biocompatibility with MC3T3-E1 cells. We found that TTC effectively released bacteriostatic agents and displayed good biocompatibility with MC3T3-E1 cells. Furthermore, our results demonstrated that UPPE/β-TCP/TTC biomaterials substantially reduced cell toxicity and increased bone-promoting effects on MC3T3-E1 cells. Finally, UPPE/β-TCP/TTC biomaterials stimulated the WNT/β-catenin pathway in these cells, which led to osteogenic differentiation. Overall, this study shed new light on the benefits of UPPE/β-TCP/TTC in promoting bone regeneration under inflammatory conditions.

2. Materials and methods

2.1 Material synthesis experiment

2.1.1 Experimental materials. Benzoyl peroxide (BPO) was purchased from Shanghai Chemical Reagent Company and recrystallized and purified using standard methods. DMA was purchased from Acros. *N*-Vinyl pyrrolidone (NVP) was purchased from Merck and purified by distillation. NaCl was purchased from Aldrich and sieved to obtain particles of 100–200 μm in diameter before use. AlamarBlue indicator was purchased from Biosource International. α-Minimum Essential Medium (α-MEM) was purchased from Biowhittaker. The Wnt/β-catenin pathway inhibitor JW67 was procured from MedChemExpress Corporation with the identifier number HY-108442. Dulbecco's modified Eagle's media (DMEM), phosphate-buffered saline (PBS), double antibodies, and trypsin were purchased from Gibco Life, and fetal bovine serum (FBS) was purchased from Gemini Bio-product company.

2.1.2 Preparation of β-TCP samples. The β-TCP powder was molded at room temperature with a molding pressure of 20 MPa and calcined at 900° for 5 h. The samples were pressed into discs of 15 mm in diameter and 1.5 mm in height, sterilized with ethylene oxide, and stored in 24-well plates under aseptic conditions.

2.1.3 Preparation of UPPE polymers and UPPE/β-TCP complexes. UPPE and β-TCP particles (100 mesh) were synthesized by Huazhong University of Science and Technology and confirmed by nuclear magnetic resonance. The samples were sterilized with ethylene oxide before use. The UPPE polymer and UPPE/β-TCP composite were made into cylindrical samples with a diameter of 15 mm and a height of 1.5 mm. They were removed after 24 h of curing, sterilized with ethylene oxide, placed in a 24-well plate after removal, and stored under aseptic conditions.

TTC was purchased as an analytical pure from Sigma (St. Louis, MO, USA). The same method was used to add 1% TTC to UPPE/β-TCP paste by weight to make two sizes of disc-shaped samples of UPPE/β-TCP complexes containing 1% tetracycline (UPPE/β-TCP + 1% TTC) with a diameter of 15 mm and a height of 1.5 mm, which were removed after 24 h of material curing, sterilized by ethylene oxide and stored under aseptic conditions for backup.

2.2 Cell culture

MC3T3-E1 cells (Riken, Hirosaka, Japan) were inoculated in T-75 flasks and cultured in α-MEM medium containing 10% (v/v) FBS and 1% (v/v) double antibodies in an incubator at 37 °C, 95% relative humidity, 5% CO_2, and changed twice a week. The cells were digested with 0.25% trypsin in the culture flask for 3 min to remove the cells from the wall. Then, the digestion was terminated by adding a fresh cell culture medium. The cells were counted under a hemocytometer, and the cell culture medium matched the cell density to the required value. The cell suspensions were added to the 24-well plates with samples prepared as described above. The wells without samples were used as blank controls, then placed in the incubator and cultured separately to start the following assays.

2.3 Cytotoxicity and proliferation experiments

2.3.1 Cytotoxicity assay of MC3T3-E1 cells. We primarily employed the direct contact method to assess the *in vitro* cytotoxicity of different material groups on MC3T3-E1 cells. The AlamarBlue method was utilized, wherein dead cells were marked red and live cells green. Initially, MC3T3-E1 cells were seeded onto the surfaces of β-TCP, UPPE polymer, UPPE/β-TCP complex, and UPPE/β-TCP + 1% TTC complex in a 24-well plate. The material-free pores were the negative control group, with a seeding density of 10 000 cells per cm^2. After incubation for 4, 8, and 15 days, the culture medium was changed every 2 days, and 10% (v/v) AlamarBlue indicator was directly added to the culture medium. The plate was then returned to the incubator and cultured for 2 hours. Subsequently, 200 μl of the reaction medium was extracted from each well, transferred to a 96-well plate, and placed in a spectrophotometer. The OD values of the experimental and hostile control groups were measured at 540 nm. The cell activity value of each material surface group was determined by calculating the ratio of the OD value of the experimental group to that of the control group. A similar method was used to calculate the cell activity values of each test group.

2.3.2 Double fluorescence staining with AO and EB. After co-culturing the materials with ME3T3-E1 cells for 4, 15, and 21 days, they were extracted from the culture plates and treated with a double fluorescent stain containing DNA embedding dyes acridine orange (AO) and ethidium bromide (EB) (PBS solution with 100 μg ml^{-1} AO and 100 μg ml^{-1} EB, pH 7.4) for 10 minutes on the surface. These stained materials were mounted on slides and examined under a fluorescence microscope (Olympus Optical, Tokyo, Japan) to simultaneously observe the survival and death of MC3T3-E1 cells anchored to the material's surface. Five samples were randomly selected from each material group and photographed using a 100× microscope in two areas. The numbers of cells in four different states were

counted: (i) cells with normal nuclei (VN, bright green chromatin with intact structure); (ii) living cells with apoptotic nuclei (VA, bright green fluorescence with highly condensed or fragmented nuclei); (iii) dead cells with normal nuclei (NVN, bright chromatin with intact structure); and dead cells with apoptotic nuclei (NVA, bright chromatin, highly condensed or fragmented). Wells without materials served as the negative control group. The percentage of live cells was calculated using the following formula to determine each material's live cell density value.

$$\text{Percentage of live cells } (\%) = \frac{\text{VN} + \text{VA}}{\text{VN} + \text{VA} + \text{NVN} + \text{NVA}} \times 100$$

2.3.3 EdU staining assay. The EdU Staining Proliferation Kit, specifically the EdU Staining Proliferation Kit (iFluor 488) (ab219801) purchased from Abcam, is designed for efficient and reliable detection of cellular proliferation through EdU staining. The main experimental steps are described below. First, culture the appropriate number of cells in a 6-well plate and allow them to grow overnight, ensuring they return to a normal state before proceeding with any necessary drug treatment or other stimulation. Next, prepare a 2× EdU working solution by diluting the 10 mM EdU stock solution to a 2× working solution (20 μM) using a 1 : 500 ratio of cell culture medium. Preheat the 2× EdU working solution (20 μM) to 37 °C and add an equal volume to the 6-well plate to achieve a final EdU concentration of 1×, for example, aiming for a final concentration of 10 μM. Subsequently, continue to culture the cells for 2 hours, followed by the completion of EdU labeling. After which, remove the culture medium and add 1 ml of fixation solution, allowing them to fix at room temperature for 15 minutes. Rinse the cells in each well three times with 1 ml of washing solution (3–5 minutes each time), before adding 1 ml of permeabilization solution to each well and incubating at room temperature for 10–15 minutes. Then, remove the permeabilization solution and wash the cells in each well 1–2 times with 1 ml of washing solution, again for 3–5 minutes each time. Following this, prepare the Click Additive Solution, and proceed to add 0.5 ml of the Click reaction mixture to each well, gently shaking the culture plate to ensure uniform coverage of the reaction mixture. Incubate at room temperature in the dark for 30 minutes. Subsequently, remove the Click reaction mixture and wash the wells three times with washing solution for 3–5 minutes each time. Finally, after staining the nuclei with DAPI, wash three times with washing solution for 3–5 minutes each time, and then mount the slides.

2.3.4 Assessment of WNT/β-catenin pathway activity. The TCF/LEF lentiviral reporter, which is tagged with the gene expressing GFP and referred to as TOP-GFP, has been extensively utilized for assessing WNT/β-catenin activity.[20] Lentivirus generated from the TCF/LEF reporter was procured from Shanghai SBO Medical Biotechnology (Shanghai, China) and used for infecting cells at the MOI of 20 for 48 hours. To evaluate WNT/β-catenin activity, the intensity of TOP-GFP was detected using fluorescent imaging.

2.4 Osteogenic potential assessment

2.4.1 Alkaline phosphatase staining (ALP) staining assay. The direct contact cultures were terminated after 8, 15, and 21 days, the medium was discarded, and two washes of PBS were performed before 400 μl of cell lysate containing 0.5% Triton-X100 was added. For most ALPs, incubation at 65 °C for 15–30 minutes will result in cell lysis, releasing cell contents into solution, which can then be suspended, cooled to room temperature, and collected. As part of the analysis, MC3T3-E1 were dispersed in Triton X-100 (Solarbio) and analyzed using an ALP activity kit (Sigma, Diagnostic Kit, Cat. No. DG1245-KALP) and a microplate reader as directed by the manufacturer. In addition, a microplate reader (SPECTROstar Nano, BMG Labtech) was used to determine the ALP activity at a wavelength of 405 nm.

2.4.2 Alizarin red S (ARS) staining assay. A 21 day cell culture experiment was conducted on MC3T3-E1 cells with various treatments to study cell mineralization. Following three rinses with PBS, the cells were fixed using 4% paraformaldehyde for 30 minutes. After being stained with alizarin red solution (1 ml per well) and fixed for 30 minutes, the mineralized nodules were observed using an inverted microscope (Leica DMi8-M GmbH). Mineralization was quantified by subjecting the samples to 10% (w/v) cetyl pyridine chlorination (Sigma-Aldrich, Merck KGaA) for 1 hour. The cell content was then measured at 560 nm using an optical density meter (Sigma-Aldrich, Merck KGaA) *via* enzyme labeling.

2.5 Immunofluorescent assay

The immunofluorescence staining procedure was conducted as per the method described in the study by Li *et al.* (2021).[20] In brief, MC3T3-E1 cells, treated with purified materials, were cultured overnight in a glass-bottomed 24-well dish and then exposed to primary antibodies (anti-β-Catenin, Cell Signaling Technology, Cat#2951, diluted at 1 : 100, anti-RUNX2, Cell Signaling Technology, Rabbit mAb#12556, diluted at 1 : 200). The cells were incubated and subsequently, a secondary antibody to Streptavidin Cy3 (Thermo Fisher Scientific, Cat#:A12421, diluted at 1 : 100) or Alexa Fluor 488 (Cat#:A21202, diluted at 1 : 100) was applied. Lastly, the nuclei were stained with DAPI dye (4′,6-diamidino-2-phenylindole, Sigma, Cat#: D9542) at room temperature for 10 minutes. Fluorescence microscopy (Olympus, Tokyo, Japan) was used to capture the images.

2.6 Scanning electron microscopy (SEM) assay

MC3T3-E1 cells were cultured on the material surface with a 10 000 cells per cm^2 density for 2 days to observe the cell morphology. Afterward, the cells were removed, washed with PBS, fixed in 2.5% glutaraldehyde buffer for 2 hours, dehydrated using graded alcohol concentrations (50%, 70%, 80%, 90%, and 100%) for 15 minutes each, and treated with isoamyl acetate for 5 minutes. The samples were then dried in a critical point desiccator (CPD030; Baltec, Bondoufle, France), gold-sprayed using a vacuum deposition system (Vacuum Desk III; Denton,

Evry, France), and observed for both surface and cell morphology using SEM.

2.7 RT-qPCR (reverse transcription quantitative PCR)

MC3T3-E1 cells were used to extract total RNA with TRIzol reagent. The obtained RNA was reverse transcribed using the TaKaRa PrimeScript RT Master Mix kit from Invitrogen. The resulting cDNA was subjected to RT-PCR using the SYBR Premixed Ex-Taq-Kit (TaKaRa) and the ABI 7300 real-time PCR system. The two-tuple Ct method determined the relative expression of glyceraldehyde-3-phosphate concerning its substrate dehydrogenase (GAPDH). The primers utilized in the present investigation for RT-qPCR analysis are delineated in Table 1.

2.8 Western blot assay

After two washes with PBS, the cells were treated with radioimmunoprecipitation buffer (Beyotime) containing 1 mmol L^{-1} phenylmethyl sulfonyl fluoride. Following a 1 minute ultrasonic shock, the MC3T3-E1 cells were centrifuged at 12 000*g* and stored at 4 °C for 10 minutes. The cell fragments were then discarded to obtain the total protein. The proteins were loaded onto a 7.5% SDS-polyacrylamide gel for electrophoresis and transferred to a polyvinylidene fluoride membrane. The membrane was incubated in 5% bovine serum albumin for 2 hours and then with primary antibodies, including ALP (1 : 1000, Abcam, ab154100), RUNX2 (1 : 1000, Abclonal, A11753), β-catenin (1 : 1000, Abcam, ab265591), phosphorylation of β-catenin (1 : 1000, Abcam, ab75777), and GAPDH (1 : 2500, Abcam, ab9485), which were incubated overnight at 4 °C. The membrane was visualized using an enhanced chemiluminescent reagent (Abcam), and GAPDH was used as an internal control. Secondary antibodies (1 : 5000, ab6721, Abcam) were applied for 2 hours in the analysis.

2.9 The release profiles of TTC from UPPE/β-TCP/TTC composite

UV-Vis spectrophotometry was utilized to monitor TCC release from the composite. The spectrophotometer employed in the study determines the concentration of a substance by measuring its absorption of light at a specific wavelength in a solution. According to Beer's law, the absorbance of a substance in a solution is directly proportional to its concentration. In the context of the drug release experiment, changes in absorbance of the sample at various time points were measured to infer the concentration variation of the drug in the solution, thus facilitating the analysis of the drug release rate. The experimental procedure involved adding 2 ml of UPPE/β-TCP/TTC complex to a 15 ml centrifuge tube and incubating it for an additional 5 minutes at 37 °C. Subsequently, the mixture was supplemented with phosphate buffered saline (PBS) to reach a total volume of 10 ml. At different time intervals, 1 ml of supernatant was collected, and an equivalent volume of fresh PBS was added in subsequent steps. The OD values were measured using a spectrophotometer (K5800, KIO, Beijing, China), and the TCC release spectrum in UPPE/β-TCP/TTC complex was determined in accordance with Lambert–Beer's law. The Lambert–Beer law, $A = Kbc$, indicates that the absorbance is directly proportional to the concentration, where A represents the absorbance value, K represents the molar absorption coefficient, b represents the optical path length, and c represents the sample concentration. Since the optical length (b) and the molar absorption coefficient (K) are constants, the absorbance value (A) varies linearly with the sample concentration (c). Subsequently, the characteristic absorbance of TCC at known concentrations was measured. This enabled the utilization of the characteristic absorbance in the UV-visible absorption spectrum of the released supernatant to determine the quantity of TCC released at different time points.

Table 1 Primer sequence of RT-qPCR[a]

Name of primer sequences (5′–3′)
Runx2 F: GGCCACTTACCACAGAGCTATTA
R: AGGCGATCAGAGAACAAACTAGG
Gapdh F: GATGCTGGTGCTGAGTATGRCG
R: GTGGTGCAGGATGCATTGCTCTGA
Alp F: TTGTGCCAGAGAAAGAGAGAGAC
R: CATACCATCTCCCAGGAACATGAT

[a] F (forward), *Gapdh* (glyceraldehyde-3-phosphate dehydrogenase), R (reverse), RT-qPCR (reverse transcription-quantitative polymerase chain reaction), *Runx2* (Runt-related transcription factor 2).

2.10 Antibacterial assay of UPPE/β-TCP/TTC materials against *P.g*

The experimental protocol for evaluating the antibacterial effect of UPPE/β-TCP/TTC materials against *P.g* is outlined as follows. Initially, the materials were immersed in PBS at 37 °C for 3 days to obtain extracts. Subsequently, *P.g* was anaerobically cultured on 5% sheep's blood agar plates supplemented with hemin (Sigma-Aldrich) and vitamin K (Yangtze River Pharmaceutical Co., Ltd, Anhui, China) for 7 days, and approximately 10^9 colony-forming units of live bacteria were dispersed in 100 μl PBS. Paper discs (6 mm) were then soaked with hydrogel extracts and placed on the inoculated agar plates. The *P.g* plates were incubated in an anaerobic environment at 37 °C for 3 days, and the diameters of the inhibition zones were measured. All experiments were performed in triplicate, with the antibacterial activity determined as the average diameter (mm) of the inhibition zones developed around the discs. Additionally, *P.g* bacterial colonies were transferred to normal and anaerobe broth medium to prepare a 10^8 CFU mL^{-1} bacterial solution. The UPPE/β-TCP/TTC materials extraction medium was utilized to investigate the antibacterial activity of the materials. Specifically, 100 μl of the bacterial stock solution was added to a 96-well plate, and a 100 μl aliquot of hydrogel extract from each group was transferred to each well and thoroughly mixed. The *P.g* plate was then incubated in an aerobic incubator at 37 °C for 3 days, and the antibacterial activity was evaluated by recording the optical density of each well at 600 nm.

2.11 Statistical analysis

Cytotoxicity, viable cell density, RT-qPCR, and ALP activity data were expressed as "mean + standard deviation", and multiple comparisons were conducted using one-way ANOVA were performed using SPSS12.0 statistical software, and $p < 0.05$ was considered statistically significant.

3. Results and discussion

3.1 Cytocompatibility of UPPE/β-TCP/TTC biocomposites

To assess the morphology of MC3T3-E1 cultured on different materials, we imaged the cell morphology cultured on four groups (β-TCP, UPPE, UPPE/β-TCP, and UPPE/β-TCP + 1% TTC) of materials using scanning electron microscopy (SEM). After 2 days of incubation, MC3T3-E1 cells could adhere and extend on the surface of the four groups. The cytoplasm of these cell protrusions contains actin microfilament bundles or actin microfilaments, with which the cells can migrate on the surface of the materials, and the cell protrusions form cell–cell bonds. In contrast, secondary protrusions on the cell protrusions continue to extend outward. We found MC3T3-E1 cells adhering tightly to the UPPE/β-TCP + 1% TTC, with secondary protrusions of about 0.1 μm in diameter at the end of MC3T3-E1 cell protrusions, and the number of secondary protrusions on the UPPE/β-TCP + 1% TTC was higher than in other groups (Fig. 1a–d). The UPPE/β-TCP + 1% TTC biocomposite was also subjected to TTC drug release detection. The drug release curve revealed a gradual increase in TTC drug release from 1 hour to 24 hours, reaching its peak at 24 hours (ESI Fig. 1†).

3.2 Biosafety of UPPE/β-TCP/TTC biocomposites

To evaluate the cytotoxicity of four groups of biocomposites (β-TCP, UPPE, UPPE/β-TCP, and UPPE/β-TCP + 1% TTC) on MC3T3-E1 cells, we conducted cytotoxicity assays to determine the cell viability of each group of materials on day 4, 8, and 15. The results demonstrated that the cell viability increased gradually in all groups of biocomposites with the increasing period of culture. Remarkably, UPPE/β-TCP + 1% TTC exhibited significantly greater cellular viability than the other three biocomposites (Fig. 2a). Moreover, we performed AO–EB double staining assay to visualize and quantify the proportion of living and dead cells on the surface of the biomaterials for immunofluorescence staining and quantitative analysis. On the fourth day of cell culture, the findings illustrated that the percentage of living cells on the surface of all four biocomposite groups exceeded 80%. The UPPE/β-TCP + 1% TTC biomaterial group displayed a notably higher percentage of living cells (over 90%) than the other three groups (Fig. 2b and c). Likewise, we performed AO/EB staining assay on cells cultured on the surface of the biocomposite for 15 days. Furthermore, the percentage of living cells on the surface of the UPPE/β-TCP + 1% TTC biocomposite was notably higher than that on the surface of the UPPE/β-TCP biocomposite group which did not contain TTC (Fig. 2d and e). Additionally, we utilized the EDU (5-ethynyl-2′-deoxyuridine) proliferation assay to determine the cellular proliferation capability on the surface of the four groups of materials on day 15. Notably, the cell proliferation capacity of the UPPE/β-TCP + 1% TTC biomaterials was significantly greater than that of the other three biomaterial groups (Fig. 2f and g). The aforementioned results demonstrated that amongst the four biomaterial groups (β-TCP, UPPE, UPPE/β-TCP, UPPE/β-TCP + 1% TTC), the biocomposite of UPPE/β-TCP + 1% TTC displayed lower toxicity towards MC3T3-E1 cells and significantly promoted its ability of proliferation.

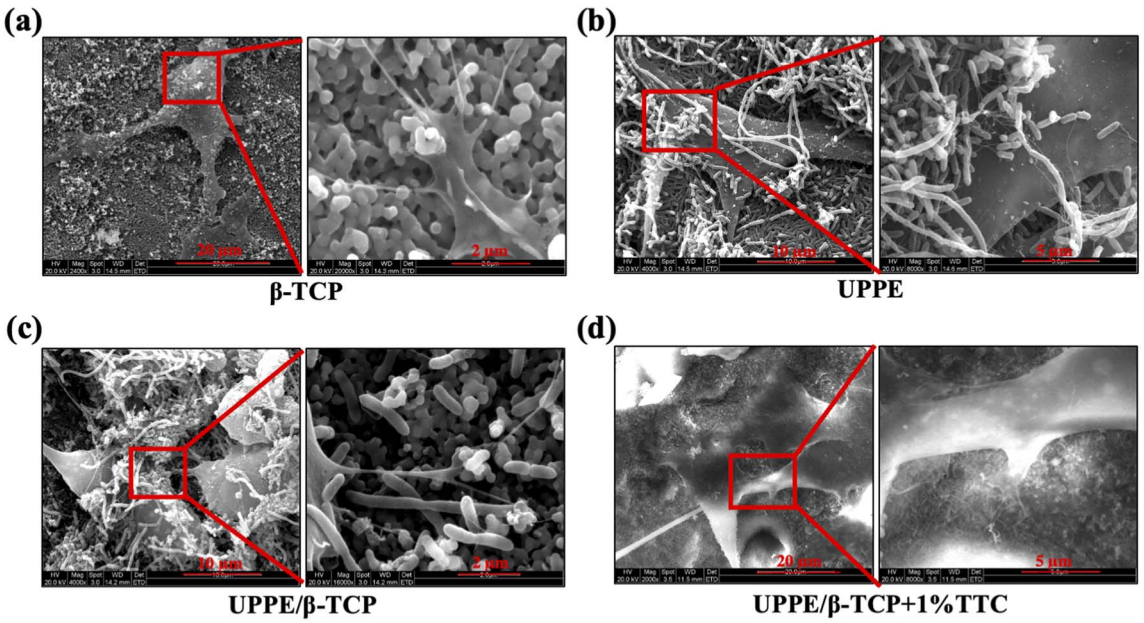

Fig. 1 The biocomposite of UPPE/β-TCP + 1% TTC demonstrates exceptional biocompatibility with MC3T3-E1 cells. SEM image of MC3T3-E1 cells adhering to the surface of β-TCP samples ((a) scale bar 20 μm and 2 μm), UPPE samples ((b) scale bar 10 μm and 5 μm), UPPE/β-TCP samples ((c) scale bar 10 μm and 2 μm), and UPPE/β-TCP + 1% TCC samples ((d) scale bar 20 μm and 5 μm).

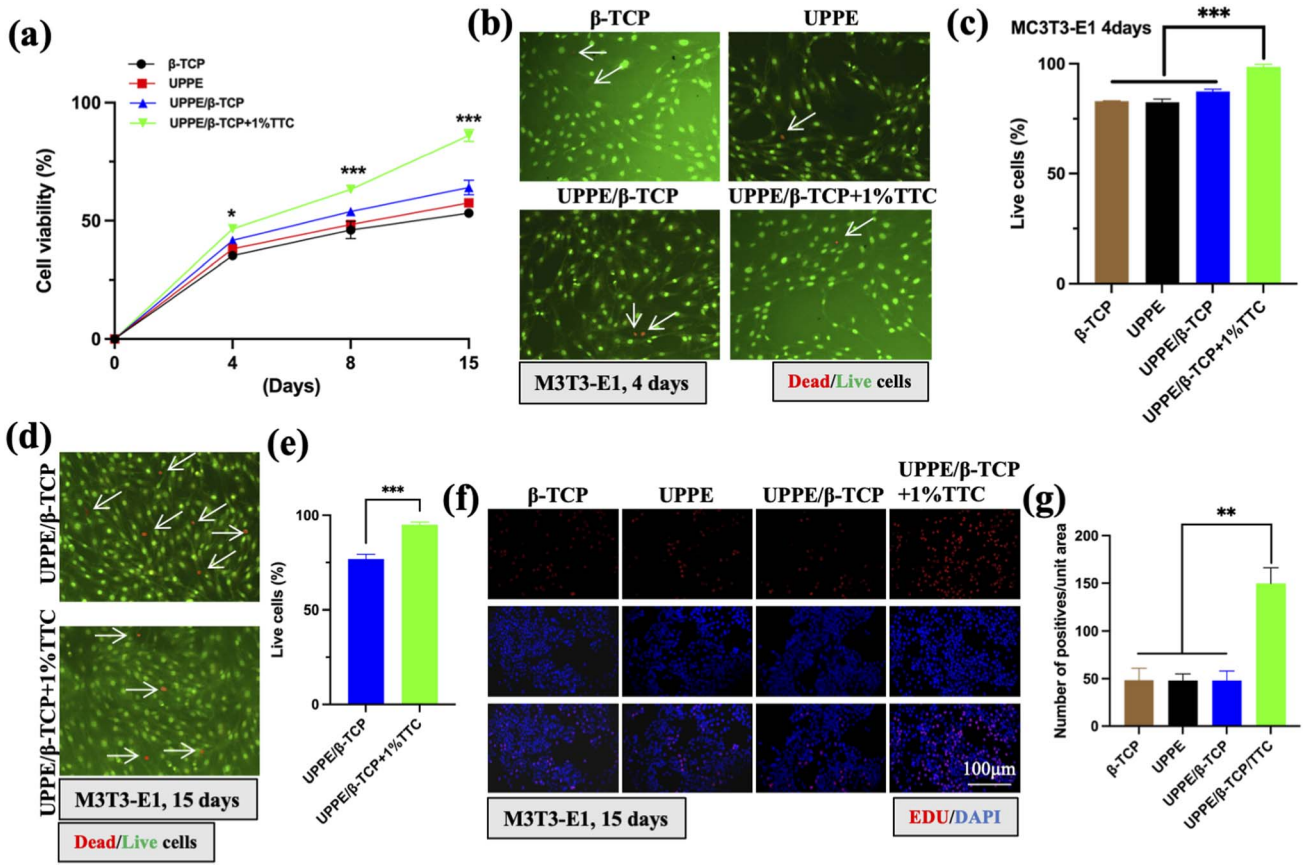

Fig. 2 The MC3T3-E1 cells exhibited higher levels of cellular activity when placed on the surface of the UPPE/β-TCP/TTC composite. (a) Cell viability of MC3T3-E1 cells cultured on β-TCP, UPPE polymer, UPPE/β-TCP, and UPPE/β-TCP + 1% TCC composite for 4, 8, and 15 days. (b) Immunofluorescent staining of live and dead cells in MC3T3-E1 on the surface of each material after cell culture for 4 days, and quantitative analysis (c). (d) Immunofluorescent staining of live and dead cells in MC3T3-E1 cells on the surface of UPPE/β-TCP and UPPE/β-TCP + 1% TTC after cell culture for 15 days, and quantitative analysis (e). (f) Immunofluorescent staining of EDU in MC3T3-E1 cells on the surface of each material after cell culture for 15 days and quantitative analysis (g). *P < 0.05, **P < 0.01, ***P < 0.001, compared with control group.

3.3 Pro-osteogenic differentiation effect of UPPE/β-TCP/TTC biocomposite

P. gingivalis (*P.g*) and its lipopolysaccharide (*P.g*-LPS) are pivotal in the onset of periodontal bone defects. As a keystone pathogen, *P.g* disrupts the oral microbial balance, causing chronic inflammation and tissue damage.[21] The potent pro-inflammatory and bone-degrading properties of *P.g*-LPS lead to the production of cytokines and matrix metalloproteinases, contributing to bone resorption. Additionally, *P.g*-LPS affects osteoblast and osteoclast activity, disrupting bone homeostasis. Understanding these intricate mechanisms is essential for developing targeted therapeutic strategies to address periodontal bone loss in the context of periodontitis.[22] To further explore the repair potential of UPPE/β-TCP + 1% TTC biocomposite on periodontitis-related bone defects. We examined the bone-promoting effect of UPPE/β-TCP + 1% TTC biomaterial on MC3T3-E1 cells under inflammatory conditions and evaluated its antibacterial effect against *P.g*. We conducted ALP activity tests on the four biocomposite groups using an ALP detection kit on days 8, 15, and 21, respectively. The results revealed that the ALP activity of UPPE/β-TCP + 1% TTC biocomposite cells was significantly higher on all three days compared to the blank control group. Furthermore, the ALP activity of the UPPE/β-TCP + 1% TTC biocomposite was significantly higher on all three days when compared to the remaining three groups (Fig. 3a). Similarly, we used RT-PCR assay to detect mRNA expression of osteogenic indicators, *ALP* and *RUNX2*, in the cells of the biocomposites. The results showed significantly higher mRNA expression of *ALP* and *RUNX2* in the UPPE/β-TCP + 1% TTC biocomposite surface cells compared to the blank control group and the remaining three groups (Fig. 3b and c). We also employed the western blot assay to detect the protein-level expression of ALP and RUNX2 in the surface cells of the biocomposites. The results showed a significantly higher expression of ALP and RUNX2 protein levels on the surface cells of UPPE/β-TCP + 1% TTC biocomposite than in the blank control group and the remaining three groups (Fig. 3d). The results indicate that UPPE/β-TCP + 1% TTC biocomposite could enhance the osteogenic potential of MC3T3-E1 cells. We conducted ARS staining experiments in the cells on the material surface to further confirm this conclusion. The results demonstrated significantly more calcium nodules in the cells on the UPPE/β-TCP + 1% TTC biocomposite group

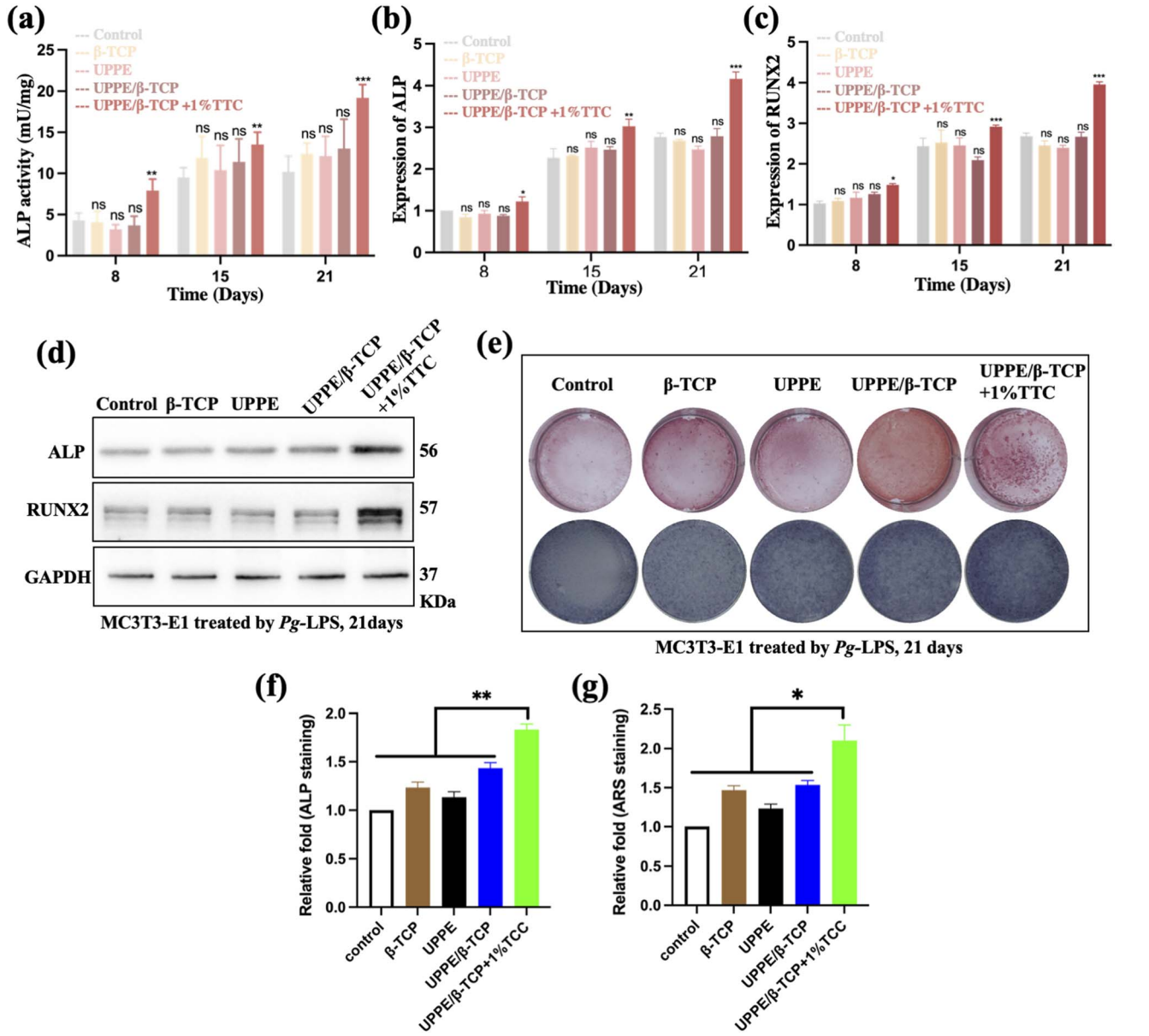

Fig. 3 The UPPE/β-TCP/TTC biocomposite significantly enhanced the *in vitro* osteogenic capacity of MC3T3-E1 cells. (a) The alkaline phosphatase (ALP) activity of MC3T3-E1 cells cultured on the surface of four materials for 8, 15, and 21 days. (b) The mRNA expression levels of *ALP* in MC3T3-E1 cells cultured on the surface of four materials for 8, 15, and 21 days. (c) The mRNA expression levels of *RUNX2* in MC3T3-E1 cells cultured on the surface of four materials for 8, 15, and 21 days. (d) The protein expression levels of ALP and RUNX2 in MC3T3-E1 cells cultured on the surface of four materials for 8, 15, and 21 days. (e) ARS staining (top row) and ALP staining (bottom row) image of MC3T3-E1 cells on the surface of UPPE/β-TCP and UPPE/β-TCP + 1% TTC after cell culture in *P.g*-LPS for 21 days, and quantitative analysis in (f, ALP staining) and (g, ARS staining). $*P < 0.05$, $**P < 0.01$, $***P < 0.001$, compared with the control group.

surface after osteogenic induction compared to the remaining three groups (Fig. 3e and f). The ALP staining results also indicated more profound staining in the cells on the surface of the UPPE/β-TCP + 1% TTC biocomposite group after osteogenesis induction (Fig. 3g and h).

3.4 UPPE/β-TCP/TTC biocomposites activate the Wnt/β-catenin pathway in the periodontitis microenvironment

To investigate the mechanism of osteogenic differentiation of MC3T3-E1 cells promoted by UPPE/β-TCP + 1% TTC composites under *P.g*-LPS stimulation, we first transfected the MC3T3-E1 cells with lentivirus (TOP-GFP) accurately reporting WNT/β-catenin pathway activity. Subsequently, the cells were treated with UPPE/β-TCP and UPPE/β-TCP + 1% TTC materials for 21 days, and the cells were harvested for immunofluorescence staining. The results showed a significantly higher expression of GFP and RUNX2 proteins in cells treated with UPPE/β-TCP + 1% TTC compared to those treated with UPPE/β-TCP alone (Fig. 4a). These findings suggest that the WNT/β-catenin pathway in MC3T3-E1 cells was activated after treatment with UPPE/β-TCP + 1% TTC. To confirm

the activation of the WNT/β-catenin pathway in MC3T3-E1 cells by treatment with UPPE/β-TCP + 1% TTC composites, we collected cells treated with UPPE/β-TCP and UPPE/β-TCP + 1% TTC biocomposites for 21 days for immunofluorescence and western blot analyses. The results showed a significant increase in the phosphorylated form of β-catenin within the nucleus of cells treated with UPPE/β-TCP + 1% TTC composites (Fig. 4b and c). We also collected MC3T3-E1 cells treated with UPPE/β-TCP + 1% TTC composites for ARS and ALP analyses after treatment with DKK1, an inhibitor of the WNT/β-catenin pathway. The results showed that osteogenic differentiation of MC3T3-E1 cells was significantly reduced when cultured on UPPE/β-TCP + 1% TTC composite (Fig. 4d–f). Additionally, we evaluated the antibacterial effects of UPPE/β-TCP and UPPE/β-TCP + 1% TTC materials on *P.g* using the agar diffusion assay. The results showed that UPPE/β-TCP + 1% TTC material had a significantly more antibacterial effect on *P.g* than UPPE/β-TCP material (ESI Fig. 2a and b†). In summary, these results suggest that UPPE/β-TCP + 1% TTC composite exhibits anti-bacterial effects and activates the Wnt/β-catenin pathway in MC3T3-E1 cells, thereby enhancing the osteogenic differentiation potential of MC3T3-E1 cells.

3.5 Discussion

The present study investigated the impact of incorporating 1% TCC into our previously developed UPPE/β-TCP biomaterials. Our findings revealed that the UPPE/β-TCP/TTC composites exhibited enhanced antibacterial properties and significantly facilitated the osteogenic differentiation potential of MC3T3-E1 cells in the presence of periodontitis-related microenvironment.

Periodontitis is a chronic inflammatory disease with multiple causes that affects the supporting structures of the teeth, destroying alveolar bone and creating horizontal and vertical bone defects.[23,24] Surgical treatments, such as bone grafts, guided bone regeneration (GBR), and guided tissue regeneration (GTR), aim at regenerating periodontal tissue to partially reconstruct tissue defects caused by periodontitis.[25,26] Despite significant progress in periodontal surgical treatment in recent decades, repairing alveolar bone defects related to periodontitis remains challenging.[27,28] This is attributed to the disadvantages of periodontal surgery, including uncontrolled infection, more significant trauma, and postoperative complications.[29] Bone tissue engineering (BTE) is a promising method for restoring bone defects through osteoprogenitor cells and scaffolds implanted *in vivo* at the bone defect site.[30] An ideal biomaterial scaffold for bone regeneration and BTE applications should possess osteoconductive, osteoinductive, and antibacterial properties.

The structure of UPPE is similar to that of biological macromolecules such as nucleic acid and phosphoric acid and the UPPE bonds in the main chain can be hydrolyzed or

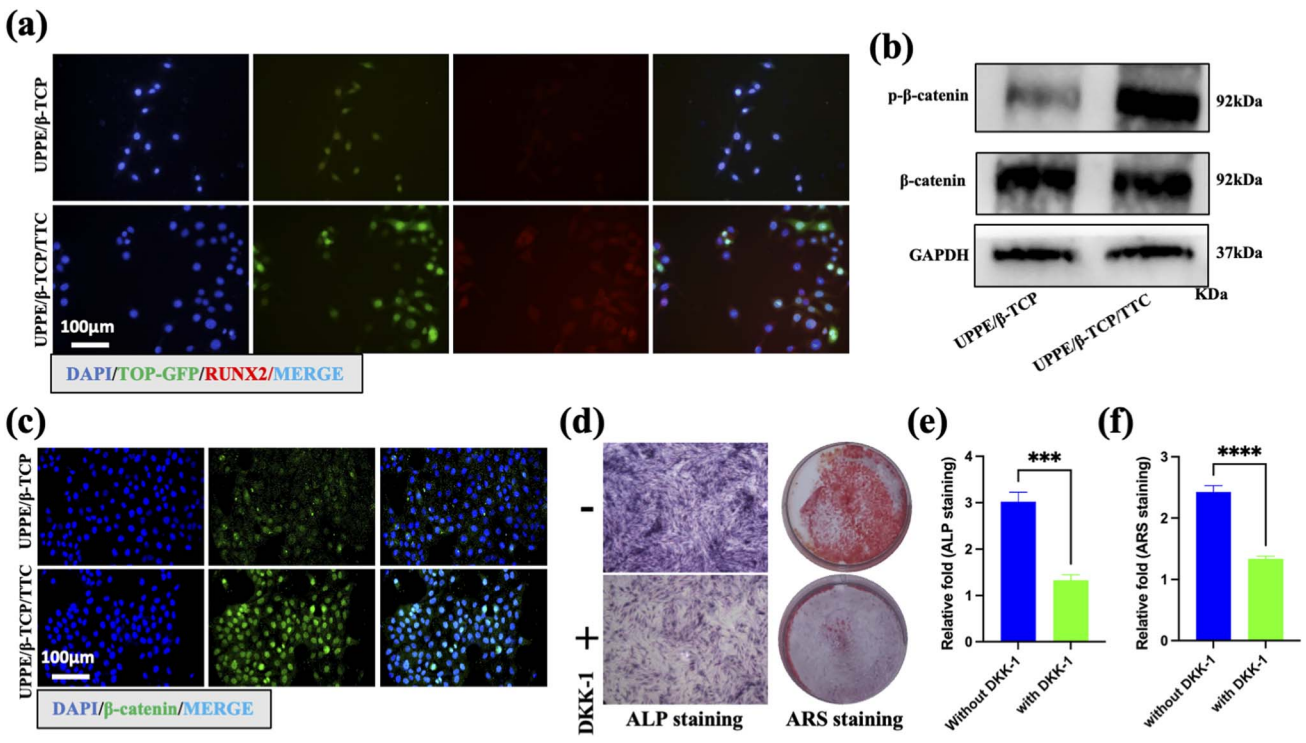

Fig. 4 UPPE/β-TCP/TTC composites enhanced the osteogenic differentiation of MC3T3-E1 cells through the Wnt/β-catenin pathway under *P.g*-LPS stimulation. (a) Immunofluorescent staining of TOP-GFP and RUNX2 in MC3T3-E1 cells on the surface of UPPE/β-TCP and UPPE/β-TCP + 1% TTC after cell culture in *P.g*-LPS for 21 days. (b) The protein expression levels of β-catenin and p-β-catenin on the surface of UPPE/β-TCP and UPPE/β-TCP + 1% TTC after cell culture in *P.g*-LPS for 21 days. (c) Immunofluorescent staining of β-catenin in MC3T3-E1 cells on the surface of UPPE/β-TCP and UPPE/β-TCP + 1% TTC after cell culture in *P.g*-LPS for 21 days. (d) ARS and ALP staining of MC3T3-E1 cells (with or without JW67, the WNT pathway inhibitors) on the surface of UPPE/β-TCP + 1% TTC after cell culture in *P.g*-LPS for 21 days and quantitative analysis in (e) and (f). ***$P < 0.001$, ****$P < 0.0001$, compared with the without JW67 group.

enzymatically degraded under physiological conditions, making the polymers with highly biodegradable and biocompatible.[31] β-TCP possesses outstanding bioactivity and biomechanical properties, thus providing robust mechanical support.[32,33] Our previous research has prepared a kind of polyphosphoester with unsaturated double bonds in the backbone by solution polymerization method, and the UPPE was prepared by cross-linking reaction with β-TCP as an inorganic filler (UPPE/β-TCP).[31,34] Nonetheless, specific issues still require attention to treat periodontal bone defects using UPPE/β-TCP biocomposite.[31] Previous studies have shown that β-TCP has good compatibility with osteoblasts.[35] This is because the main component of bone tissue is hydroxyapatite, which, like β-TCP, is composed of calcium and phosphate ions. Therefore, in this study, the custom-made β-TCP exhibits good biocompatibility with osteoblasts, allowing MC3T3-E1 cells to attach, grow, and proliferate well on its surface. Both the UPPE/β-TCP composite and UPPE/β-TCP + 1% TTC composite degrade *in vitro* cell culture medium, but at a significantly slower rate than UPPE polymer. Additionally, the β-TCP fillers in these composites have good hydrophilicity and can release a considerable amount of Ca^{2+} ions into the cell culture medium, partially or completely neutralizing the acidic degradation products of UPPE polymer, thereby acting as a buffer. As a result, these composites exhibit lower cytotoxicity upon contact with MC3T3-E1 cells, explaining the slightly higher *in vitro* cell viability observed in composites containing β-TCP compared to UPPE polymer alone.

TTC is a commonly used antibiotic in clinical practice.[36] Besides its antibacterial properties, TTC exhibits various special effects including anti-inflammatory, anti-ulcer, and promoting bone tissue regeneration.[37] Although TTC, a fermentation product of the *Streptomyces aureofaciens* bacteria discovered as early as 1948, research on TTC has continued to the present day. In this study, the addition of 1% TTC to the UPPE/β-TCP composite maintained consistently high levels of ALP activity throughout the entire culture period, with statistically significant differences observed compared to the other groups. It is well-known that when osteoclast activity increases, lysosomes in the cells release collagenase, cathepsin K, and hydrolytic enzymes, which digest the organic components of the bone matrix. TTC can decrease osteoclast activity, exert anti-collagenase activity, prevent a decrease in mineral density, and stimulate new bone formation.[38] Therefore, the addition of TTC to the UPPE/β-TCP composite promotes early functional expression when osteoblast cells come into contact with the material surface, which is beneficial for early healing of bone defects. Additionally, the cells' ability to synthesize bone matrix on or within the material allows for the integration of the bone implant with the bone tissue over time, promoting the growth of bone tissue.[39] In recent years, researchers have conducted several studies on the application of TTC in the repair of periodontitis-related bone defects, yielding significant advances.[40] For instance, studies have demonstrated that TTC can alleviate the symptoms of periodontitis by exerting anti-inflammatory effects and facilitating localized tissue repair.[41] TTC can inhibit inflammatory responses and cartilage resorption, thereby mitigating the infiltration and destruction of inflammatory cells and consequently mitigating bone destruction and bone defects.[42] Moreover, TTC can promote bone matrix synthesis, enhance bone cell function, and contribute to the reparation of bone defects caused by periodontitis.[43] According to the study by Zhao *et al.*,[44] greater surface hydrophilicity in materials can lead to enhanced osteoblast differentiation. The findings of this experiment demonstrated a gradual increase in ALP activity of MC3T3-E1 cells on the surface of the UPPE/β-TCP composite, peaking on the 21st day. The osteogenic differentiation of MC3T3-E1 cells on the surfaces of the UPPE polymer and UPPE/β-TCP composite was reminiscent of the results obtained by Peter *et al.*,[45] in their study of PPF polymer and PPF/β-TCP composite. Their research revealed that primary rat bone marrow stromal cells expressed low levels of ALP markers on both the PPF polymer and the PPF/β-TCP composite during the initial 2 weeks but displayed significant increases in the subsequent 2 weeks, indicating that the PPF/β-TCP composite exhibits similar *in vitro* bone conduction properties to polystyrene culture plates. Consequently, the addition of β-TCP as a filler in UPPE polymer has the potential to increase ALP activity and promote significant differentiation of MC3T3-E1 cells into osteoblast cell lines without compromising the osteogenic properties of UPPE.

Typically, the integration of bone substitutes with bone tissue is evaluated through histological examinations using animal models. However, this method requires a large number of experimental animals and the standardization of experiments is challenging, making it difficult to compare materials. Given the crucial role of osteoblasts in bone defect repair, extensive research has been conducted on the interaction between osteoblasts and implants. Among these studies, the MC3T3-E1 cell line is one of the most commonly used cell models. Numerous studies have demonstrated that this non-transformed cell line exhibits high alkaline phosphatase (ALP) activity *in vitro*, promoting extracellular matrix mineralization. Additionally, factors such as material composition, surface morphology, and surface energy significantly influence the initial adhesion, spreading, and expression of differentiation markers in MC3T3-E1 cells. Hence, the MC3T3-E1 osteoblast cell line serves as a valuable model for studying the attachment, proliferation, and differentiation of osteoblasts on bone substitute surfaces. Considering these factors, this study selected the MC3T3-E1 osteoblast cell line and utilized non-toxic standard polyethylene culture plates as the negative control group to investigate the biological behavior of osteoblasts on custom-made alveolar bone repair materials, including their effects on cell viability, morphology, adhesion, and differentiation. Our findings indicate that the addition of 1% TTC to UPPE/β-TCP material demonstrates a significant reduction in cytotoxicity, as well as improvements in cytocompatibility, biocompatibility, and osteogenic differentiation potential of MC3T3-E1 cells (Fig. 1–3). These results highlight the favorable biosafety profile and effective cell-hosting capability of our optimized biocomposite, UPPE/β-TCP + 1% TTC. Our finding indicates that TTC exhibits promising potential in the repair of bone defects caused by periodontitis. However, the

present state of research is in its nascent stage, necessitating further clinical trials and investigations to determine the safety and efficacy of tetracycline in repairing periodontitis-related bone defects and to refine treatment strategies further.

The Wnt/β-catenin pathway is a crucial signaling pathway that plays a vital role in embryonic development, cell proliferation, differentiation, and tissue regeneration.[46] Under normal conditions, β-catenin is continuously degraded, maintaining a low intracellular level.[20,47] However, upon binding the Wnt protein to the Frizzled receptor, intracellular β-catenin is stabilized, translocates into the nucleus, binds to transcription factors, and enhances gene transcription, thereby regulating various biological processes.[48] In recent years, the Wnt/β-catenin pathway has been identified as a pivotal player in regenerating periodontal bone defects.[49,50] Experimental evidence suggests that activation of the Wnt/β-catenin pathway enhances bone tissue regeneration in periodontal bone defects.[51] Specifically, activation of the Wnt/β-catenin pathway stimulates backbone cell proliferation and differentiation, enhances bone matrix synthesis and deposition, and promotes new bone formation.[41] Moreover, the Wnt/β-catenin pathway regulates inflammation, immune response, and apoptosis, thereby positively affecting the treatment and regeneration of periodontal bone defects.[49] However, despite the significant role played by the Wnt/β-catenin pathway in periodontal bone defects, there is still a need for further investigation to elucidate its underlying regulatory mechanism and specific functions.[52] The present study yielded unexpected findings, demonstrating a substantial enhancement in the osteogenic potential of MC3T3-E1 cells cultured on the UPPE/β-TCP/TCC biocomposite surface (Fig. 3) accompanied by a significant activation of the Wnt/β-catenin pathway (Fig. 4a–c). Concurrently, upon inhibiting the activity of the Wnt/β-catenin pathway using inhibitors, a notable attenuation in the osteogenic differentiation-promoting effect of the UPPE/β-TCP/TCC biocomposite on MC3T3-E1 cells was observed (Fig. 4d–f). These findings partially support the crucial role of the Wnt/β-catenin pathway in the repair of periodontal bone defects. However, further investigation is needed for the specific molecular mechanism of UPPE/β-TCP/TCC material in activating the Wnt/β-catenin pathway.

4. Conclusions

In this study, the UPPE/β-TCP/TTC composites exhibited favorable biosafety and cytocompatibility *in vitro*. Furthermore, within the microenvironment of periodontitis, the UPPE/β-TCP/TTC composite effectively stimulated the Wnt/β-catenin pathway of MC3T3-E1 cells, consequently promoting its osteogenic differentiation. These findings present a novel biomaterial and therapeutic approach for addressing periodontitis-related bone defects.

Author contributions

All of the authors contributed to the preparation of the manuscript. Z-X. Z. proposed the experimental direction of this research, and J. M. proposed the theoretical direction of this research. Z-X. Z. and Q-L. L. developed the UPPE/β-TCP/TTC composites. Q-L. L., Y-X. W. and Y-X. Z. investigated the experimental background of the UPPE/β-TCP/TTC composites, performed experiments, and prepared the figures.

Conflicts of interest

There are no conflicts of interest to declare.

Acknowledgements

This work was mainly supported by the Natural Science Foundation of Hubei Province (2022CFB293) and Tongji Hospital Fund Cultivation Project (2023B16). We also thank Prof. Shiqiang Gong for discussing our research results.

References

1 M. Jiang, Z. Li and G. Zhu, *Oral Dis.*, 2020, **26**, 259–269.
2 F. Kimura, K. Miyazawa, K. Hamamura, M. Tabuchi, T. Sato, Y. Asano, S. Kako, Y. Aoki, Y. Sugita, H. Maeda, A. Togari and S. Goto, *Life Sci.*, 2021, **284**, 119938.
3 N. Ahmad, F. J. Ahmad, S. Bedi, S. Sharma, S. Umar and M. A. Ansari, *Saudi Pharm. J.*, 2019, **27**, 778–790.
4 Y. Yamada, S. Nakamura-Yamada, R. Konoki and S. Baba, *Stem Cell Res. Ther.*, 2020, **11**, 175.
5 M. G. Balta, E. Papathanasiou, I. J. Blix and T. E. Van Dyke, *J. Dent. Res.*, 2021, **100**, 798–809.
6 C. Garot, G. Bettega and C. Picart, *Adv. Funct. Mater.*, 2020, **31**(5), 2006967.
7 J. He, X. Hu, J. Cao, Y. Zhang, J. Xiao, L. Peng, D. Chen, C. Xiong and L. Zhang, *Carbohydr. Polym.*, 2021, **253**, 117198.
8 C. C. Liu, A. Solderer, C. Heumann, T. Attin and P. R. Schmidlin, *J. Dent.*, 2021, **114**, 103812.
9 Y. Yu, Y. Wang, W. Zhang, H. Wang, J. Li, L. Pan, F. Han and B. Li, *Acta Biomater.*, 2020, **113**, 317–327.
10 M. Ferri, S. Campisi, L. Polito, J. Shen and A. Gervasini, *J. Hazard. Mater.*, 2021, **420**, 126656.
11 Y. Lai, Y. Li, H. Cao, J. Long, X. Wang, L. Li, C. Li, Q. Jia, B. Teng, T. Tang, J. Peng, D. Eglin, M. Alini, D. W. Grijpma, G. Richards and L. Qin, *Biomaterials*, 2019, **197**, 207–219.
12 L. M. Golub and H. M. Lee, *Periodontol. 2000*, 2020, **82**, 186–204.
13 M. Kaur, M. Nagpal and M. Singh, *Curr. Drug Targets*, 2020, **21**, 1640–1651.
14 L. M. Golub, N. Ramamurthy, T. F. McNamara, B. Gomes, M. Wolff, A. Casino, A. Kapoor, J. Zambon, S. Ciancio, M. Schneir, *et al.*, *J. Periodontal Res.*, 1984, **19**, 651–655.
15 L. M. Golub, J. M. Goodson, H. M. Lee, A. M. Vidal, T. F. McNamara and N. S. Ramamurthy, *J. Periodontol.*, 1985, **56**(Suppl 11S), 93–97.
16 T. Ingman, T. Sorsa, K. Suomalainen, S. Halinen, O. Lindy, A. Lauhio, H. Saari, Y. T. Konttinen and L. M. Golub, *J. Periodontol.*, 1993, **64**, 82–88.

17 G. J. Boelen, L. Boute, J. d'Hoop, M. EzEldeen, I. Lambrichts and G. Opdenakker, *Clin. Oral Invest.*, 2019, **23**, 2823–2835.
18 L. Wang, F. Wu, Y. Song, X. Li, Q. Wu, Y. Duan and Z. Jin, *Cell Death Dis.*, 2016, **7**, e2327.
19 Q. Shao, S. Liu, C. Zou and Y. Ai, *Oral Dis.*, 2023, **29**, 1137–1148.
20 Q. Li, D. Xia, Z. Wang, B. Liu, J. Zhang, P. Peng, Q. Tang, J. Dong, J. Guo, D. Kuang, W. Chen, J. Mao, Q. Li and X. Chen, *Front. Cell Dev. Biol.*, 2021, **9**, 656981.
21 G. Hajishengallis, *Nat. Rev. Immunol.*, 2015, **15**, 30–44.
22 R. J. Lamont and G. Hajishengallis, *Trends Mol. Med.*, 2015, **21**, 172–183.
23 F. Lei, M. Li, T. Lin, H. Zhou, F. Wang and X. Su, *Acta Biomater.*, 2022, **141**, 333–343.
24 M. Sanz, A. Marco Del Castillo, S. Jepsen, J. R. Gonzalez-Juanatey, F. D'Aiuto, P. Bouchard, I. Chapple, T. Dietrich, I. Gotsman, F. Graziani, D. Herrera, B. Loos, P. Madianos, J. B. Michel, P. Perel, B. Pieske, L. Shapira, M. Shechter, M. Tonetti, C. Vlachopoulos and G. Wimmer, *J. Clin. Periodontol.*, 2020, **47**, 268–288.
25 A. B. Novaes Jr and D. B. Palioto, *Periodontol. 2000*, 2019, **79**, 56–80.
26 D. F. Kinane, P. G. Stathopoulou and P. N. Papapanou, *Nat. Rev. Dis. Primers*, 2017, **3**, 17038.
27 M. Aljateeli, T. Koticha, J. Bashutski, J. V. Sugai, T. M. Braun, W. V. Giannobile and H. L. Wang, *J. Clin. Periodontol.*, 2014, **41**, 693–700.
28 B. Pretzl, S. Salzer, B. Ehmke, U. Schlagenhauf, B. Dannewitz, H. Dommisch, P. Eickholz and Y. Jockel-Schneider, *Clin. Oral Invest.*, 2019, **23**, 3073–3085.
29 J. Gargallo-Albiol, S. Barootchi, O. Salomo-Coll and H. L. Wang, *Ann. Anat.*, 2019, **225**, 1–10.
30 M. Alonzo, F. A. Primo, S. A. Kumar, J. A. Mudloff, E. Dominguez, G. Fregoso, N. Ortiz, W. M. Weiss and B. Joddar, *Curr. Opin. Biomed. Eng.*, 2021, **17**, 100248.
31 Z. Zhang, X. Feng, J. Mao, J. Xiao, C. Liu and J. Qiu, *Biochem. Biophys. Res. Commun.*, 2009, **379**, 557–561.
32 S. K. Lee, C. M. Han, W. Park, I. H. Kim, Y. K. Joung and D. K. Han, *Mater. Sci. Eng., C*, 2019, **94**, 65–75.
33 M. Bohner, B. L. G. Santoni and N. Dobelin, *Acta Biomater.*, 2020, **113**, 23–41.
34 Z. Zhang, J. Mao, X. Feng, J. Xiao and J. Qiu, *J. Huazhong Univ. Sci. Technol., Med. Sci.*, 2008, **28**, 604–607.
35 A. Ehara, K. Ogata, S. Imazato, S. Ebisu, T. Nakano and Y. Umakoshi, *Biomaterials*, 2003, **24**, 831–836.
36 T. A. Seregina, I. Y. Petrushanko, R. S. Shakulov, P. I. Zaripov, A. A. Makarov, V. A. Mitkevich and A. S. Mironov, *Cells*, 2022, **11**(17), 2667.
37 A. J. Warner, J. D. Hathaway-Schrader, R. Lubker, C. Davies and C. M. Novince, *Bone*, 2022, **159**, 116377.
38 M. E. Ryan, R. A. Greenwald and L. M. Golub, *Curr. Opin. Rheumatol.*, 1996, **8**, 238–247.
39 Y. Zhang, K. Li, L. Shen, L. Yu, T. Ding, B. Ma, S. Ge and J. Li, *ACS Appl. Mater. Interfaces*, 2022, **14**, 268–277.
40 J. E. Rojas-Paulus, G. G. P. Manfredi, S. Salmeron, A. Consolaro, A. C. P. Sant'Ana, M. S. R. Zangrando, C. A. Damante, S. L. A. Greghi and M. L. R. Rezende, *J. Periodontol.*, 2021, **92**, 678–688.
41 X. Zheng, S. Wang, L. Xiao, P. Han, K. Xie, S. Ivanovski, Y. Xiao and Y. Zhou, *J. Periodontal Res.*, 2022, **57**, 835–848.
42 G. S. Chatzopoulos, V. P. Koidou and L. Tsalikis, *Clin. Oral Invest.*, 2023, **27**, 955–970.
43 M. Laster, R. C. Pereira and I. B. Salusky, *Bone*, 2019, **127**, 114–119.
44 G. Zhao, Z. Schwartz, M. Wieland, F. Rupp, J. Geis-Gerstorfer, D. L. Cochran and B. D. Boyan, *J. Biomed. Mater. Res., Part A*, 2005, **74**, 49–58.
45 S. J. Peter, L. Lu, D. J. Kim and A. G. Mikos, *Biomaterials*, 2000, **21**, 1207–1213.
46 P. Duan and L. F. Bonewald, *Int. J. Biochem. Cell Biol.*, 2016, **77**, 23–29.
47 G. Shen, H. Ren, Q. Shang, W. Zhao, Z. Zhang, X. Yu, K. Tang, J. Tang, Z. Yang, D. Liang and X. Jiang, *EBioMedicine*, 2020, **52**, 102626.
48 S. J. Schunk, J. Floege, D. Fliser and T. Speer, *Nat. Rev. Nephrol.*, 2021, **17**, 172–184.
49 X. L. Han, M. Liu, A. Voisey, Y. S. Ren, P. Kurimoto, T. Gao, L. Tefera, P. Dechow, H. Z. Ke and J. Q. Feng, *J. Dent. Res.*, 2011, **90**, 1312–1317.
50 W. T. Oh, Y. S. Yang, J. Xie, H. Ma, J. M. Kim, K. H. Park, D. S. Oh, K. H. Park-Min, M. B. Greenblatt, G. Gao and J. H. Shim, *Mol. Ther.*, 2023, **31**, 435–453.
51 D. Cui, N. Kong, L. Ding, Y. Guo, W. Yang and F. Yan, *Adv. Healthcare Mater.*, 2021, **10**, e2101215.
52 Q. Zhai, X. Chen, D. Fei, X. Guo, X. He, W. Zhao, S. Shi, J. J. Gooding, F. Jin, Y. Jin and B. Li, *Adv. Sci.*, 2022, **9**, e2103839.